Check for updates

JGR Biogeosciences

RESEARCH ARTICLE
10.1029/2021JG006629

Reduced Soil Gross N_2O Emission Driven by Substrates Rather Than Denitrification Gene Abundance in Cropland Agroforestry and Monoculture

Jie Luo[1], Lukas Beule[2], Guodong Shao[1], Edzo Veldkamp[1], and Marife D. Corre[1]

[1]Soil Science of Tropical and Subtropical Ecosystems, Faculty of Forest Sciences and Forest Ecology, University of Goettingen, Goettingen, Germany, [2]Julius Kühn Institute (JKI)—Federal Research Centre for Cultivated Plants, Institute for Ecological Chemistry, Plant Analysis and Stored Product Protection, Berlin, Germany

Key Points:

- The tree row in the agroforestry decreased annual gross N_2O emission and increased annual gross N_2O uptake compared to monoculture
- Reduced gross N_2O emission was directly regulated by mineral N, C availability, and WFPS rather than denitrification gene abundance
- The increased gross N_2O uptake in the agroforestry was largely controlled by the low mineral N-to-CO_2-C ratio in the tree row

Supporting Information:

Supporting Information may be found in the online version of this article.

Correspondence to:

J. Luo and M. D. Corre,
jluo@gwdg.de; LuoJ0616@hotmail.com
mcorre@gwdg.de

Citation:

Luo, J., Beule, L., Shao, G., Veldkamp, E., & Corre, M. D. (2022). Reduced soil gross N_2O emission driven by substrates rather than denitrification gene abundance in cropland agroforestry and monoculture. *Journal of Geophysical Research: Biogeosciences*, *127*, e2021JG006629. https://doi.org/10.1029/2021JG006629

Received 16 SEP 2021
Accepted 21 FEB 2022

Abstract Conversion of monoculture to agroforestry (integrating trees with crops) is promoted as a promising management in reducing N_2O emissions from croplands. How agroforestry influences gross N_2O emission ($N_2O + N_2$ from N_2O reduction) and uptake (N_2O reduced to N_2) compared to monoculture is unknown. We used the $^{15}N_2O$ pool dilution technique to quantify these processes using soil cores (top 5 cm) incubated in the field with monthly measurements over two growing seasons (2018–2019) at two sites (each with paired agroforestry and monoculture) and one site with monoculture only. The unfertilized tree rows showed the lowest gross N_2O emissions ($P \leq 0.002$). Although tree rows occupied only 20% in agroforestry, gross N_2O emissions tended to decrease by 6–36% in agroforestry (0.98–1.02 kg N_2O-N ha^{-1} yr^{-1}) compared to monoculture (1.04–1.59 kg N_2O-N ha^{-1} yr^{-1}). Gross N_2O emissions were influenced by soil mineral N, soil respiration, and moisture content rather than by denitrification gene abundance. Soil gross N_2O uptake was highest in the tree row and decreased with distance into crop rows ($P = 0.012$). The agroforestry tended to increase gross N_2O uptake by 27–42% (0.38–0.44 kg N_2O-N ha^{-1} yr^{-1}) compared to monoculture (0.30–0.31 kg N_2O-N ha^{-1} yr^{-1}). In tree rows, soil gross N_2O uptake correlated with *nirK* gene abundance which was indirectly influenced by the low mineral N-to-soil CO_2-C ratio. Adjusting the tree and crop areal coverages of agroforestry and optimizing fertilization can further augment the benefits of agroforestry in reducing emission and increasing uptake of N_2O in soils.

Plain Language Summary Nitrous oxide (N_2O) is a potent greenhouse gas and its largest anthropogenic source is from nitrogen fertilization in agriculture. Conversion of cropland monoculture to agroforestry (integrating trees with crops) is one promising mitigation practice to reduce soil N_2O emissions from agriculture. We quantified gross rates of N_2O emission ($N_2O + N_2$ from N_2O reduction) and uptake (N_2O reduced to N_2) in the soil to evaluate how agroforestry performs compared to monoculture. Our findings showed that agroforestry decreased gross N_2O emissions and increased gross N_2O uptake. These were due to the absence of nitrogen fertilization and increased soil respiration (which partly indicated increase in carbon availability to soil microbes) in the tree row. These findings suggest that if fertilizer inputs are optimized without sacrificing crop yield or profit, combined with the impact of tree rows on increasing soil N_2O uptake, agroforestry will be an efficient mitigation strategy to curb N_2O emissions from croplands. The benefits of agroforestry in reducing gross N_2O emission and increasing gross N_2O uptake in soils should be included in the economic valuation to support its policy implementation and adoption by farmers.

1. Introduction

Nitrous oxide (N_2O) is an important ozone-depleting substance and a potent greenhouse gas (GHG) with 265 times global warming potential relative to CO_2 in a 100-year time frame (IPCC, 2014). The main source of N_2O is croplands, which occupy about 12% of the Earth's ice-free land (Foley et al., 2011). Soil N_2O emissions from croplands have increased from 0.3 Tg N_2O-N yr^{-1} in the preindustrial period to 3.3 Tg N_2O-N yr^{-1} in recent decades (2007–2016), accounting for 82% of the global N_2O increase (Tian et al., 2018), as a result of cropland expansion and increased N fertilizer use to meet the food demand of the growing human population (IPCC, 2019). Therefore, meeting the goal of keeping global warming below 2°C by 2,100 requires the adoption of a set of strategies to reduce detrimental impacts of increasing N fertilizer use in agriculture on the environment (Galloway et al., 2008).

© 2022. The Authors.
This is an open access article under the terms of the Creative Commons Attribution-NonCommercial-NoDerivs License, which permits use and distribution in any medium, provided the original work is properly cited, the use is non-commercial and no modifications or adaptations are made.

Agroforestry, that is, simultaneous cultivation of trees and crops in arable land, is promoted as one of the promising strategies to mitigate climate change and reduce nutrient leaching losses while maintaining agricultural productivity (Smith et al., 2013). Modern agroforestry systems in the temperate zone include alley-cropping systems that alternate rows of trees with rows of crops, whereby fast-growing trees (e.g., *Populus nigra* × *P. maximowiczii*) are used for feedstock of bioenergy production (Schmidt et al., 2021). These systems have been shown to be profitable (Langenberg et al., 2018) and deliver ecosystem services such as carbon (C) sequestration (Ma et al., 2020; Pardon et al., 2017), biodiversity improvement (Banerjee et al., 2016; Beule & Karlovsky, 2021), food production and security (Beaudette et al., 2010; Beule, Lehtsaar et al., 2019; Schmidt et al., 2021), and climate mitigation (Chapman et al., 2020; Wolz et al., 2018). Few studies in the temperate zone suggest that cropland agroforestry reduces soil N_2O emissions (Amadi et al., 2016, 2017; Beaudette et al., 2010). These studies, however, focused mainly on net soil N_2O flux (e.g., using the static chamber method), which is the net balance of the simultaneously occurring processes of gross production and gross consumption of N_2O in soils. Net N_2O flux measurement does not allow us to delve into the mechanisms driving N_2O production and consumption. The Intergovernmental Panel on Climate Change has included the net N_2O uptake by soils in the global N_2O budget in 2013, showing that this sink is possibly more important than previously assumed (Chapuis-Lardy et al., 2007). A recent review showed that one-third of studies conducted in terrestrial ecosystems in the past decades (1975–2015) reported both N_2O and N_2 fluxes, but 84% of these were conducted only in the laboratory (Almaraz et al., 2020). It is therefore imperative to quantify separately gross N_2O production and consumption for systematic comparison between cropland agroforestry and monoculture in order to fill the knowledge gap of field-based quantification of gross N_2O fluxes in response to land use/management change.

Moreover, quantifying the relationships of gross N_2O production and consumption with controlling factors will advance our predictive understanding of the soil N_2O flux dynamics (Sihi et al., 2020; Yang & Silver, 2016a). The $^{15}N_2O$ pool dilution ($^{15}N_2O$ PD) technique enables the simultaneous measurement of gross N_2O fluxes without extensive soil disturbance (e.g., Wen et al., 2016; Yang et al., 2011). Previous studies that applied this method denoted the terms "gross N_2O production" and "gross N_2O consumption" (Yang et al., 2011; Yang & Silver, 2016a, 2016b). Later, however, Wen et al. (2016) had compared the gas-flow soil core method (Butterbach-Bahl et al., 2002) with the $^{15}N_2O$ PD technique, and their values differed. This suggests that while $^{15}N_2O$ PD method quantifies gross rates of N_2O emitted and reduced within interconnected soil pores, it may have excluded anaerobic microsites (e.g., soil microspots saturated with water, isolated pores filled with or enclosed by water, and water-entrapped N_2O) which are not in direct exchange with the soil air (Figure S1 in Supporting Information S1). Thus, Wen et al. (2016) proposed to use the terms "gross N_2O emission and uptake" when employing the $^{15}N_2O$ PD technique, as we used in our present study. So far, gross N_2O emission and uptake have only been investigated in a few land use systems: temperate forest (Wen et al., 2017), managed grassland (Yang et al., 2011), cropland, and salt marsh landscape (Yang & Silver, 2016a, 2016b).

Denitrification and nitrification are the main sources of N_2O in the soil, while denitrification is the only known soil-borne sink of N_2O (i.e., N_2O reduction to N_2, catalyzed by N_2O reductase that is encoded by the *nos* gene cluster; Chapuis-Lardy et al., 2007; Juhanson et al., 2017). Previous studies on gross N_2O emission and uptake reported that soil mineral N and available C are the main controls in a forest (Wen et al., 2017) and a fertilized corn cropland (Yang & Silver, 2016b). Soil moisture and temperature regulate gross N_2O fluxes through their effects on gas diffusion and their redox influence on microbial N and C cycling processes (e.g., Butterbach-Bahl et al., 2013; Davidson et al., 2000; Müller & Sherlock, 2004). Moreover, soil texture, management practices associated with crop types or trees (i.e., agroforestry), and climate influence those small-scale regulating factors by altering available N and C levels, soil moisture, and microbial community composition (Beule & Karlovsky, 2021; Lang et al., 2019; Mitchell et al., 2020; Strickland et al., 2015). At our present study sites, agroforestry tree rows reduce wind speed and result in low evapotranspiration (Kanzler et al., 2019; Markwitz et al., 2020), which may maintain higher soil moisture compared to cropland monoculture. At the same study sites, agroforestry tree rows are unfertilized (Beule et al., 2020; Schmidt et al., 2021), and thus have a low soil mineral N but large N response efficiency due to the trees' high biomass production (Schmidt et al., 2021). As opposed to the commonly fertilized crop rows of agroforestry and monocultures, the high litter inputs in the agroforestry tree rows may lead to a lower mineral N-to-available C ratio, which favors N_2O reduction to N_2 (Weier et al., 1993). Also, Beule et al. (2020) found that tree rows promote the population size of denitrifying microorganisms relative to monoculture, suggesting a greater potential for complete denitrification (with N_2 as the end product) under the trees as compared to cropland monoculture. At present, there is lacking quantitative assessment of the relationships among gross

N_2O fluxes, substrate levels, soil moisture and temperature conditions, and denitrification gene abundance in response to management change (i.e., monoculture to agroforestry); such field-based quantitative relationships may improve biogeochemical models at a large scale.

Our objectives were to: (a) quantify gross N_2O emission and gross N_2O uptake in cropland agroforestry and monoculture systems, and (b) assess the relationship of gross N_2O fluxes with soil controlling factors, including a suite of denitrification gene abundance (*nirK*, *nirS*, *nosZ* clades), during two growing seasons at three sites on different soils in Germany. We hypothesized that (a) cropland agroforestry will have lower gross N_2O emission and higher gross N_2O uptake than monocultures, and (b) this pattern of gross N_2O fluxes will reflect the changes in substrate levels, soil moisture, and temperature conditions as well as in denitrifier population size. Our findings provide support on GHG regulation function for policy implementation of agroforestry.

2. Materials and Methods

2.1. Study Sites and Experimental Design

Our study was conducted at three sites in Germany, of which two sites had paired cropland agroforestry and monoculture on a loam Calcaric Phaeozem soil (at Dornburg, Thuringia) and a clay Vertic Cambisol soil (at Wendhausen, Lower Saxony) and one site was a cropland monoculture on a sandy Arenosol soil (at Vechta, Lower Saxony; Figure 1a; soil characteristics in Table S1 in Supporting Information S1). Hereafter, we refer to these study sites by their soil types, based on FAO World Reference Base soil classification. The cropland agroforestry systems at the two sites were established by converting cropland monoculture into poplar-based alley-cropping systems. At each site, the crops of the adjacent cropland agroforestry and monoculture were managed identically (i.e., the same crops, fertilization period and rates, and cultivation and harvesting methods; Table 1), and the monoculture served as the reference land use prior to agroforestry conversion. The two cropland agroforestry systems were established in 2007 at the site with a Phaeozem soil and in 2008 at the site with a Cambisol soil. Each agroforestry system consisted of 12-m wide poplar (poplar clone max 1; *Populus nigra* × *P. maximowiczii*) rows planted by hand from cuttings and 48-m wide crop rows in a north-south orientation, commonly done to minimize differences in light availability (Pardon et al., 2018; Swieter et al., 2019). The aboveground tree biomass of the agroforestry systems in the Phaeozem and Cambisol soils was harvested for biofuel at the beginning of 2015 and 2014 (Table 1), respectively. The regrown poplar trees at these two agroforestry sites were 4–5 years old during our study period (from March 2018 to September 2019). The crop rotations at the three study sites included summer barley (*Hordeum vulgare*), winter oilseed rape (*Brassica napus*), winter wheat (*Triticum aestivum*), rye (*Secale cereale*), corn (*Zea mays*), and potato (*Solanum tuberosum*; Table 1). Fertilization was generally applied in spring to cropland monocultures and agroforestry crop rows. The agroforestry tree rows were not fertilized, as commonly practiced in temperate agroforestry systems (Schmidt et al., 2021; Tsonkova et al., 2012).

Four replicate plots were established at each of the cropland agroforestry and monoculture systems in the Phaeozem and Cambisol soils, and eight replicate plots were established in the cropland monoculture in the Arenosol soil. Each replicate plot in the cropland agroforestry represented a transect spanning from the center of the tree row into the center of the crop row to capture a spatial gradient induced by the tree rows. Each of these transects had four sampling locations: at the center of tree row and from the tree row at 1, 7, and 24 m within the crop row (Figure 1b). In the field, we observed that the fertilizer broadcaster drove at 12 m from the tree row; the fertilizers were broadcasted for the entire 12 m length at each side, and the broadcaster turned around for the remaining 24 m crop row to be fertilized. At midway (24 m) of the agroforestry crop row, the fertilizers were broadcasted with about 1 m overlapped, such that at the middle of this crop row, the amount of fertilizers were possibly more than the rest of the length of the crop row. In the cropland monocultures, measurements were carried out at the center of each replicate plot (Figure 1b). Thus, on each monthly sampling, there were 20 measurements in the Phaeozem and Cambisol soils (4 replicate plots in the agroforestry × 4 sampling locations + 4 replicate plots in the monoculture), and eight measurements in the Arenosol soil (8 replicate plots in the monoculture).

2.2. Measurement of Gross N_2O Emission and Uptake

Gross N_2O emission and gross N_2O uptake were measured monthly from March 2018 to September 2019 in the field, using the $^{15}N_2O$ PD technique as described by Wen et al. (2016, 2017) and adapted from Yang et al. (2011). At each of the four sampling locations per replicate plot of the agroforestry or at each replicate plot in the

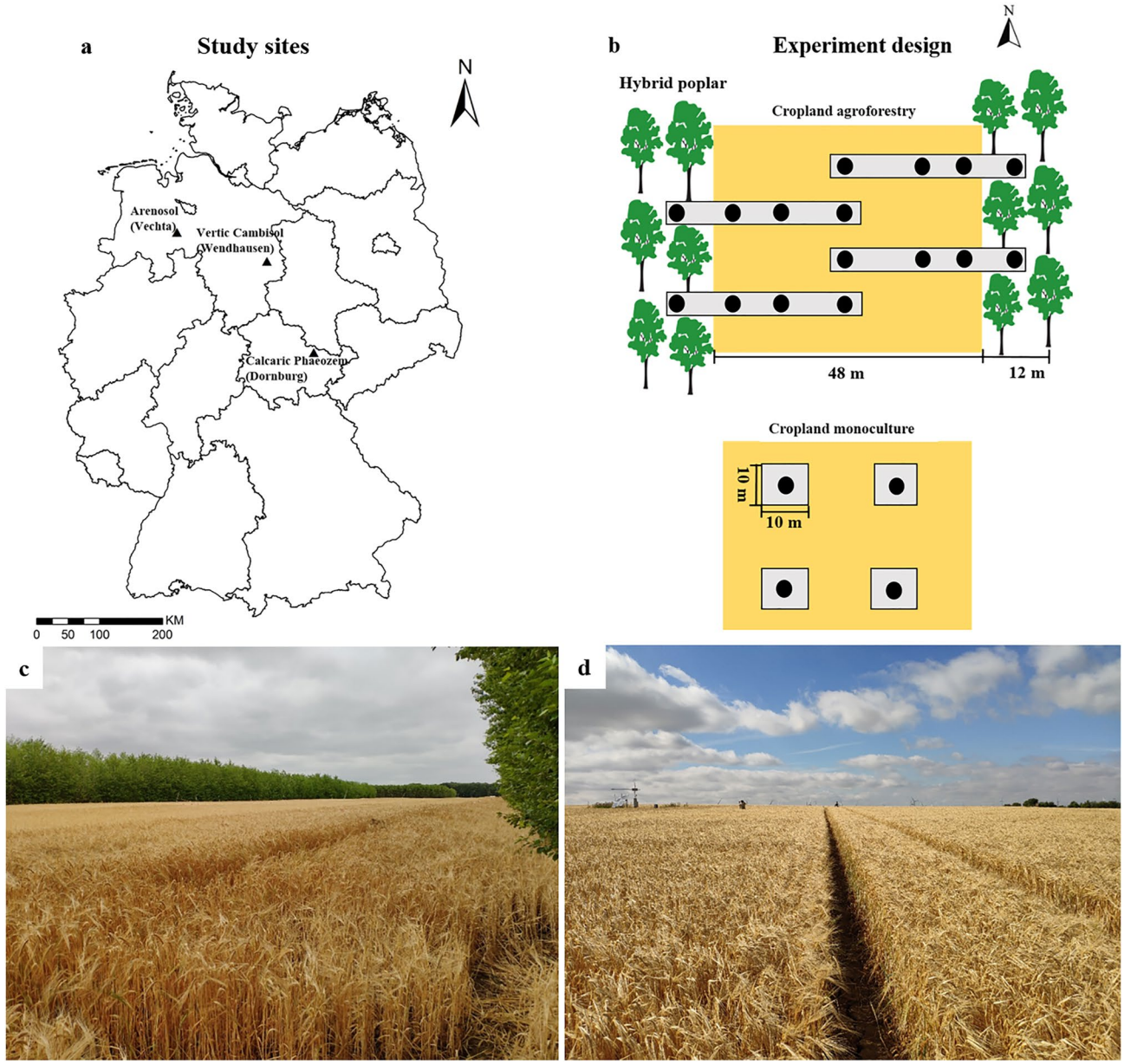

Figure 1. (a) Locations of the three study sites in Germany. (b) The layout of the experimental design: ● indicate sampling locations (in the cropland agroforestry, each replicate plot (▭) was sampled at the tree row, 1-m, 7-m, and 24-m distances from the tree row; in the cropland monoculture, measurements were taken in the center of each replicate plot). (c) Cropland agroforestry and (d) monoculture at Dornburg in the Phaeozem soil (picture credit: G. Shao).

monoculture systems, four intact 250-cm^3 soil cores of the top 5-cm depth were collected and placed in an air-tight chamber (glass desiccator of 6.6 L volume), equipped with a Luer-lock stopcock on the lid (Figure S2 in Supporting Information S1), for immediate incubation in the field. We injected 7 mL of $^{15}N_2O$ label gas into the chamber headspace, which was composed of 100 ppm_v of 98% single labeled ^{15}N-N_2O, 275 ppb_v sulfur hexafluoride (SF_6, as a tracer for possible physical loss of gases from the chamber headspace) and balanced with synthetic air (Westfalen AG, Münster, Germany). This label gas resulted in initial headspace concentrations of approximately 125 ppb_v N_2O with 13.2% ^{15}N initial enrichment and 344 ppt_v SF_6. Based on conservative calculations, the diffusion of labeled $^{15}N_2O$ through the 5 cm long soil cores shows that the labeled $^{15}N_2O$ diffuses into the soil and back to the headspace within 0.5 hr (Wen et al., 2016). Thus, our sampling of the chamber headspace at 0.5 hr and thereafter hourly during a 3-hr in situ incubation was sufficient to allow a homogeneous mixture of $^{15}N_2O$ with soil-derived N_2O. At 0.5, 1, 2, and 3 hr in situ incubation, gas samples of 100 and 23 mL were taken from

Table 1
Site Characteristics and Management Practices at Three Sites of Cropland Agroforestry and Cropland Monocultures in Germany

Study site	Dornburg	Wendhausen	Vechta
Soil type	Calcaric Phaeozem	Vertic Cambisol	Arenosol
Location	51°00′40″N, 11°38′46″E	52°20′00″N, 10°37′55″E	52°45′29″N, 8°32′5″E
Mean Annual Air Temperature			
Long-term (2010–2019)	10.7 ± 0.3°C[a]	10.7 ± 0.3°C[b]	10.1 ± 0.1°C[c]
Study period (2018–2019)	11.5 ± 0.1°C[a]	11.5 ± 0.1°C[b]	10.9 ± 0.1°C[c]
Mean Annual Precipitation			
Long-term (2010–2019)	567 ± 32 mm[a]	587 ± 41 mm[b]	643 ± 35 mm[c]
Study period (2018–2019)	450 ± 35 mm[a]	479 ± 99 mm[b]	577 ± 157 mm[c]
Elevation (m above sea level)	289	82	38
Year of agroforestry establishment	2007	2008	None
Harvest of the aboveground tree biomass in the agroforestry	January 2015	January 2014	None
Crops rotation in 2016–2017–2018–2019	Summer barley-winter oilseed rape-winter wheat-summer barley	Winter oilseed rape-winter wheat-winter wheat-corn	Corn-potato-rye-corn
Sowing and harvest of the crops	October 2017 July 2018	October 2017 July 2018	October 2017 July 2018
	March 2019 July 2019	April 2019 October 2019	April 2019 September 2019
Fertilization rates in 2018 and 2019 (kg N-P-K ha^{-1} yr^{-1})	213-0-0 (2018)	166-0-116 (2018)	188-26-108 (2018)
	36-22-31 (2019)	101-0-0 (2019)	153-54-62 (2019)

[a]Climate station at Jena (station ID: 2444). [b]Braunschweig (station ID: 662). [c]Diepolz (station ID: 963) of the German Meteorological Service.

the chamber headspace and injected respectively into a preevacuated 100-mL glass bottle and 12-mL glass vial (Exetainer; Labco Limited, Lampeter, UK) with rubber septa (Figure S2 in Supporting Information S1). To maintain the headspace at atmospheric pressure and oxygen concentration, the sampled air volume at each time was replaced by a 123 mL gas mixture of 80% helium and 20% oxygen (v/v) so as not to change the ^{15}N-N_2O isotope composition in the headspace (Wen et al., 2016, 2017). The dilution caused by this replacement was accounted for in the calculations. The 100-mL gas samples were analyzed for isotopic composition using an isotope ratio mass spectrometer (Finnigan Delta^{plus} XP, Thermo Electron Corporation, Bremen, Germany). The 23-mL gas samples were analyzed for N_2O and SF_6 concentrations, using a gas chromatograph (SRI 8610C, SRI Instruments Europe GmbH, Bad Honnef, Germany) with an electron capture detector (and a make-up gas of 5% CO_2-95% N_2, 5.0 purity grade), as well as for CO_2 concentrations using the same gas chromatograph but with a methanizer and flame ionization detector. During each in situ incubation, air temperature, and pressure were measured as well as ambient air samples were taken (23 mL for determination of ambient N_2O concentration and 100 mL for analysis of natural abundance $^{15}N_2O$ signatures) to be used for the gross N_2O flux calculations. Atmospheric N_2O concentration was 345.9 ± 0.5 ppb_v and ^{15}N natural abundance was 0.3691 ± 0.0001 atom% across the three sites over the 1.5-year measurement period. Details on the principles and calculations of gross N_2O emission and uptake were given in our earlier works (Wen et al., 2016, 2017). Net soil N_2O and CO_2 fluxes were calculated from the linear increase of their concentrations during the incubation period and adjusted with the measured air temperature and pressure (e.g., Matson et al., 2017).

Gross N_2O, net N_2O, and soil CO_2 fluxes were expressed on the dry mass of intact soil cores, determined from the concurrently measured gravimetric moisture content (see Section 2.3). Annual soil gross N_2O fluxes from each sampling location at each replicate plot were calculated by trapezoidal interpolation between fluxes and sampling day intervals from March 2018 to February 2019 (e.g., Koehler et al., 2009; Matson et al., 2017; Veldkamp et al., 2013). The annual fluxes were converted from mass-basis to area-basis for the top 5-cm depth, using the measured soil bulk density (see Section 2.3), which was averaged for each site (1.0 g cm^{-3} for the Phaeozem and Cambisol soils, and 1.3 g cm^{-3} for the Arenosol soil).

For the agroforestry system as a whole, gross N_2O fluxes at each replicate plot were weighted by the areal coverages of the tree row and the crop row sampling locations. The weighting factors were calculated by considering half of the widths of the tree row (6 m) and the crop row (24 m), totaling to 30 m, since these alternating tree and crop rows indicated that half of their widths represented each side of the rows (Figure 1b). Considering the 1-m width overlap of the fertilizer broadcaster at 24 m (see above), we calculated the overall values for agroforestry in two ways. First, only considering the weighting factors of the tree row (0.2, for 6 m/30 m), 1 m (0.13, for 4 m/30 m), and 7 m (0.67, for 20 m/30 m). Second, we included the 24 m using a weighting factor of 0.07 (for 2 m/30 m) and adjusting the weighting factor of the 7 m to 0.6 (for 18 m/30 m). This weighting factor of 24 m was derived by a 1-m increment adjustment between the 7 and 24 m, and we found that the statistical results did not change regardless of the adjusted weighting factors between these two sampling locations.

2.3. Soil Controlling Factors

Following the measurement of the gross N_2O fluxes, soil controlling factors (temperature, WFPS, nitrate [NO_3^-], ammonium [NH_4^+], and denitrification genes *nirK*, *nirS*, *nosZ* clades I and II, see Section 2.4) were all determined from the soil cores on each sampling day. Additionally, microbial biomass C and N were measured at a quarterly interval from the soil cores following gross N_2O flux measurements. The gravimetric moisture content (oven-drying soil sample at 105°C for 1 day) was expressed in WFPS using the average bulk density (determined from one of the four soil cores used for the monthly measurements of gross N_2O fluxes) for each soil type (or site) and the mineral soil particle density of 2.65 g cm^{-3}. The remaining three soil cores were pooled, mixed thoroughly in the field and a subsample was immediately put into a pre-weighed extraction bottle containing 150 mL 0.5 M K_2SO_4 for the determination of extractable mineral N. Additionally, a subsample of approximately 20 g soil was directly transferred to a sterile 15-mL polypropylene Falcon tube and frozen at −20°C in the field for DNA extraction and quantification of denitrification genes (see Section 2.4). Upon arrival at the laboratory, extraction bottles were shaken for 1 hr, filtered, and the extracts were frozen immediately until further analysis. Microbial biomass C and N were determined using the chloroform fumigation-extraction method (Brookes et al., 1985) by fumigating about 20 g fresh soil for 5 days, followed by extraction with 100 mL 0.5 M K_2SO_4. The dry mass of the extracted fresh soils as well as the fumigated soils was calculated using the concurrently measured gravimetric moisture content. Microbial biomass C and N were calculated as the difference in the extractable C and total extractable N between the paired fumigated and unfumigated soils divided by k_C and k_N factors of 0.45 and 0.68, respectively (Shen et al., 1984). Extractable organic C concentration was measured using ultraviolet-enhanced persulfate oxidation using a Total Organic Carbon Analyzer (TOC-Vwp, Shimadzu Europa GmbH, Duisburg, Germany). The extractable mineral N (NH_4^+, NO_3^-) and total extractable N concentrations were analyzed using continuous flow injection colorimetry (SEAL Analytical AA3, SEAL Analytical GmbH, Norderstedt, Germany), where NH_4^+ was determined by salicylate and dichloroisocyanuric acid reaction, NO_3^- by cadmium reduction method with NH_4Cl buffer and total extractable N by ultraviolet-persulfate digestion followed by hydrazine sulfate reduction.

General soil characteristics in the top 30 cm (pH, total N, organic C, effective cation exchange capacity, base saturation, and clay content) were determined using standard methods as described in our previous work (Schmidt et al., 2021; Table S1 in Supporting Information S1).

2.4. Quantification of Denitrification Genes in Soil

Denitrification genes were quantified in the Phaeozem and Cambisol soils from the thoroughly mixed soils of the cores used for gross N_2O flux measurement, and these were frozen immediately in the field. Frozen soils were freeze-dried for 72 hr and subsequently homogenized using a swing mill (MM400, Retsch, Haan, Germany) at 25 Hz for 1 min. Soil DNA was extracted from 50 mg finely ground freeze-dried soil, using a modified protocol of Brandfass and Karlovsky (2008), as described previously (Beule, Corre, et al., 2019). Briefly, the soil was suspended in 1 mL cetyltrimethylammonium bromide buffer with proteinase K. The mixture was incubated at 42°C and subsequently at 65°C for 10 min each, and 800 µL phenol was added. The mixture was shaken, centrifuged and the supernatant was extracted twice with chloroform/isoamylalcohol. DNA from the obtained supernatant was precipitated using polyethylene glycol/NaCl, pelleted using centrifugation, washed twice with 80% (w/v) EtOH, and dried using a vacuum centrifuge. The dried pellets were resuspended in 50 µL TE buffer (10 mM Tris/HCl, 1 mM EDTA, pH 8.0). Extraction success was verified on agarose gels. Soil DNA extracts were tested for

PCR inhibitors as described previously (Guerra et al., 2020) and diluted in 1:50 double-distilled H_2O to overcome inhibitory effects on PCR.

Nitrite (NO_2^-) reductase (*nirK* and *nirS*) and N_2O reductase genes (*nosZ* clades I and II) were quantified using real-time PCR (qPCR), as described previously (Beule, Corre, et al., 2019). Briefly, denitrification genes were amplified from diluted soil DNA extracts in a CFX 384 Thermocycler (Biorad, Rüdigheim, Germany) using 4 µL reaction volume. The reaction volume contained Standard *Taq* Reaction Buffer (New England Biolabs, Beverly, Massachusetts, USA; 10 mM Tris-HCl, 50 mM KCl, 1.5 mM $MgCl_2$, pH 8.3 at 25°C) adjusted to different final concentrations of $MgCl_2$ (Table S2 in Supporting Information S1), 100 µM of each deoxyribonucleoside triphosphate, 0.5 or 1.0 µM of each primer (Table S2 in Supporting Information S1), 1 µg/µL bovine serum albumin, 0.03 u/µL Hot Start Taq DNA Polymerase (New England Biolabs, Beverly, Massachusetts, USA), 0.1 × SYBR Green I solution (Invitrogen, Karlsruhe, Germany) and 1 µL template DNA or in double-distilled H_2O for negative controls. Primer choice and thermocycling conditions are listed in Table S3 in Supporting Information S1.

2.5. Statistical Analysis

First, we tested each parameter for normal distribution using Shapiro-Wilk's test and for equality of variance using Levene's test. Parameters with nonnormal distribution or unequal variances were either logarithmically (i.e., soil CO_2 fluxes, total mineral N [sum of NO_3^- and NH_4^+], *nirK*, *nirS*, *nosZ* clades I and II) or cube-root transformed (i.e., gross N_2O emission, gross N_2O uptake, and microbial biomass N). Linear mixed-effect (LME) models were used to assess the differences between agroforestry and monocultures at each site with management system as fixed effect or the differences among cropland monocultures with soil type as fixed effect; sampling day and replicate plot were considered as random effects (Crawley, 2007). These LME models were extended to include either (a) a variance function (varIdent) that allow variance heteroscedasticity of the fixed effect, and/or (b) a first-order temporal autoregressive function that assumes decreasing autocorrelation between sampling days with increasing time difference (Zuur et al., 2009) if this improved the relative goodness of the model fit based on the Akaike information criterion. To evaluate the differences in gross rates of N_2O fluxes between the agroforestry as a whole and the monoculture, the agroforestry was weighted by the areal coverage of the agroforestry sampling locations and LME was conducted as above. Annual fluxes from March 2018 to February 2019 were not tested statistically for differences between agroforestry and monoculture since these values are trapezoidal extrapolations.

To assess the temporal relationships between concurrently measured soil gross N_2O fluxes and soil variables, we carried out a stepwise analysis: first within each management system at each site, and then across management systems and sites when the relationships were similar. We used the average of the four (for Phaeozem and Cambisol soils) or eight plots (Arenosol soil) on each monthly measurement and conducted Pearson correlation as well as regression analyses over the entire measurement period. The 95% confidence interval of the regression parameters is provided for an estimate of dispersion. Across sites, the total number of observations (n) was 167; the Phaeozem soil had $n = 75$ (i.e., 15 monthly measurements × 4 sampling locations in the agroforestry + 15 monthly measurements in monoculture), the Cambisol soil had $n = 80$ (i.e., 16 monthly measurements × 4 sampling locations in the agroforestry + 16 monthly measurements in monoculture), and the Arenosol soil had $n = 12$ (12 monthly measurements in monoculture). For the denitrification genes, these were measured in the Phaeozem and Cambisol soils, and hence $n = 155$. The combined effects of soil variables (which are not autocorrelated based on Pearson correlation tests) on gross N_2O fluxes were assessed using a stepwise multiple regression with forward variable selection. We conducted this multiple regression analysis separately for agroforestry and monoculture systems, with the purpose that such regression relationships may be useful in adapting predictive models for similar temperate land use management. All statistical tests were considered significant at $P \leq 0.05$. We conducted all statistical analyses using R version 3.6.3 (R Core Team, 2019).

3. Results

3.1. Gross N_2O Fluxes

Peaks of gross N_2O emissions in crop rows of agroforestry and monoculture (Figures 2a–2c) corresponded to the periods of fertilization in spring when WFPS was high (Figures S3a–S3c in Supporting Information S1) and soil temperature was increasing (Figures S3d–S3f in Supporting Information S1). Gross N_2O emissions from the

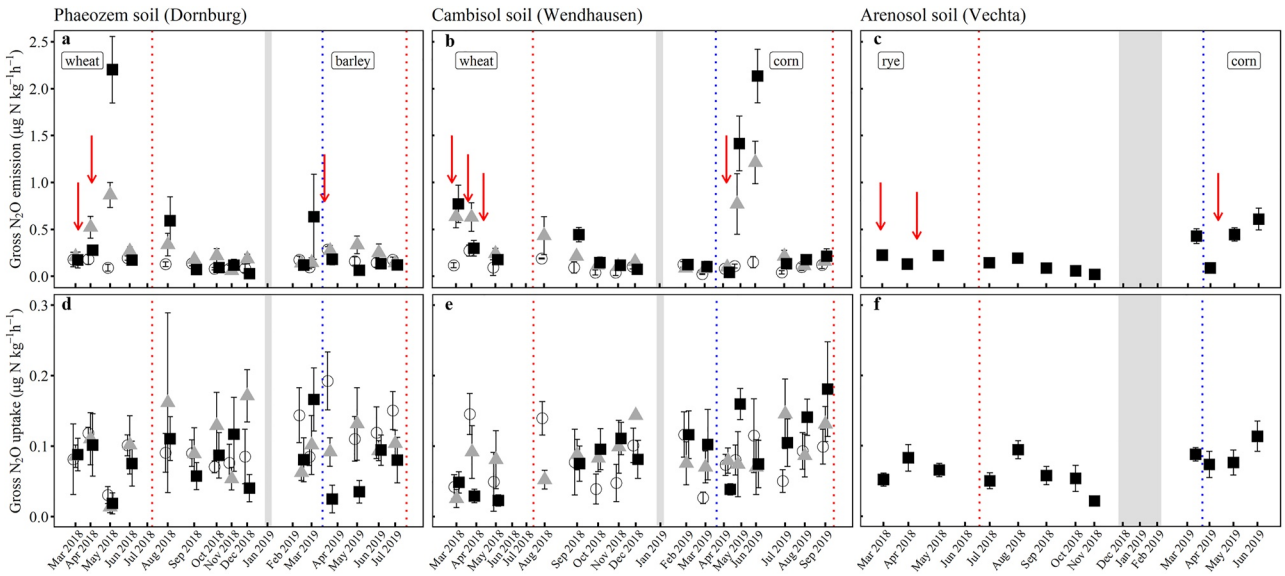

Figure 2. Mean (±SE, $n = 4$ plots for the Phaeozem and Cambisol soils, $n = 8$ plots for the Arenosol soil) gross rates of soil N_2O emission (upper panels, a, b, c) and uptake (lower panels, d, e, f), measured monthly in the top 5-cm depth using $15N_2O$ pool dilution technique at three sites of cropland agroforestry and cropland monocultures in Germany. Agroforestry tree row (○) and crop row (area-weighted average of the 1-m, 7-m, and 24-m sampling locations, (▲); monoculture (■). The site with an Arenosol soil was a cropland monoculture during the measurement period. June and July 2018 were extremely dry months, during which intact soil cores cannot be collected. Red dotted lines indicate harvest and blue dotted lines indicate sowing; gray shadings indicate frozen soil during winter when intact soil cores cannot be collected; red arrows indicate fertilizer applications in the agroforestry crop row (tree rows are commonly not fertilized) and the monocultures (fertilization rates are in Table 1).

agroforestry were lower in the tree row than in the crop row in both Phaeozem and Cambisol soils ($P \leq 0.002$; Table 2). Despite slight decreases in gross N_2O emissions in agroforestry as a whole (area-weighted by the tree and crop rows), these did not differ from the monocultures ($P \geq 0.15$; Table 2). Among the cropland monocultures, the clay Cambisol soils had larger gross N_2O emissions than the sandy Arenosol soil ($P = 0.006$; Table 2).

On the other hand, no clear seasonal pattern of gross N_2O uptake was observed at our sites (Figures 2d–2f). Gross N_2O uptake was higher in the tree row than in the center of the crop row in the Phaeozem soil ($P = 0.012$; Table 2), and the entire agroforestry showed higher N_2O uptake than the monoculture ($P = 0.046$; Table 2). This pattern was not statistically significant in the Cambisol soil ($P = 0.31$; Table 2).

3.2. Soil Variables

In the loam Phaeozem and clay Cambisol soils, WFPS was highest in the tree rows, followed by the crop rows and lowest in the monocultures ($P \leq 0.003$; Table 3). At these sites, WFPS ranged from 21% to 67% during spring, from 22% to 45% during summer, and from 23% to 65% during fall (Figures S3a and S3b in Supporting Information S1). The monoculture in the sandy Arenosol soil had the lowest WFPS ($P < 0.001$; Table 3), ranging from 19% to 46% during spring, 18–23% during summer, and 26–30% during fall (Figure S3c in Supporting Information S1). Soil temperature neither differed between management systems nor among sites, ranged from 7.1 to 25.2°C during spring, from 15.7 to 29.2°C during summer, and from −0.5 to 18.6°C during fall (Figures S3d–S3f in Supporting Information S1). In the Phaeozem and Cambisol soils, soil respiration showed a similar seasonal pattern as the WFPS and temperature (Figures S3g–S3i in Supporting Information S1). Soil respiration was larger in the tree rows than in the crop rows and monocultures ($P \leq 0.014$; Table 3) whereas mineral N showed the converse pattern ($P \leq 0.011$; Table 3). Ratios of mineral N-to-soil CO_2-C in the Phaeozem and Cambisol soils, respectively, were: 4 ± 0 and 8 ± 1 in the agroforestry tree rows, 38 ± 1 and 112 ± 20 in the crop rows, and 101 ± 19 and 147 ± 28 in the monoculture. In the Phaeozem and Cambisol soils, microbial biomass C and N decreased with increasing distance from the tree row into the crop row ($P \leq 0.048$; Table 3) whereas the monocultures showed intermediate values ($P \geq 0.68$). The monoculture in Arenosol soil had the lowest microbial biomass C and N ($P < 0.001$; Table 3).

Table 2
Mean (±SE, n = 4 Plots for the Phaeozem and Cambisol Soils, n = 8 Plots for the Arenosol Soil) and Annual Gross Rates of Soil N_2O Emission and Uptake Across Monthly Measurements From March 2018 to September 2019 in the Top 5-cm Depth, Measured Using $^{15}N_2O$ Pool Dilution Technique, at Three Sites of Cropland Agroforestry and Cropland Monocultures in Germany

Soil type (site; Crop)	Management system	Gross N_2O emission (μg N kg^{-1} h^{-1})	Gross N_2O uptake (μg N kg^{-1} h^{-1})	Annual gross N_2O emission (kg N ha^{-1} yr^{-1})	Annual gross N_2O uptake (kg N ha^{-1} yr^{-1})
Phaeozem (Dornburg; 2018—Wheat; 2019—Barley)	Tree row	0.15 ± 0.02^{b}	0.10 ± 0.02^{a}	0.54 ± 0.05	0.38 ± 0.04
	1 m crop row	0.21 ± 0.06^{b}	0.09 ± 0.02^{ab}	0.98 ± 0.27	0.37 ± 0.06
	7 m crop row	0.27 ± 0.07^{ab}	0.11 ± 0.03^{ab}	1.17 ± 0.15	0.48 ± 0.10
	24 m crop row	0.46 ± 0.12^{a}	0.07 ± 0.02^{b}	2.22 ± 0.39	0.27 ± 0.03
	Agroforestry	0.24 ± 0.05^{A} (0.25 ± 0.05^{A})	0.10 ± 0.02^{A} (0.10 ± 0.02^{A})	1.02 ± 0.08 (1.09 ± 0.07)	0.44 ± 0.06 (0.43 ± 0.06)
	Monoculture	0.33 ± 0.16^{abA}	0.08 ± 0.02^{abB}	1.59 ± 0.26	0.31 ± 0.02
Cambisol (Wendhausen; 2018—Wheat; 2019—Corn)	Tree row	0.11 ± 0.01^{b}	0.08 ± 0.01^{a}	0.53 ± 0.07	0.38 ± 0.05
	1 m crop row	0.31 ± 0.05^{a}	0.09 ± 0.00^{a}	1.42 ± 0.46	0.38 ± 0.03
	7 m crop row	0.33 ± 0.03^{a}	0.09 ± 0.01^{a}	0.99 ± 0.04	0.38 ± 0.03
	24 m crop row	0.40 ± 0.06^{a}	0.11 ± 0.01^{a}	1.34 ± 0.09	0.42 ± 0.05
	Agroforestry	0.27 ± 0.08 A (0.28 ± 0.08 A)	0.08 ± 0.01 A (0.09 ± 0.01 A)	0.96 ± 0.06 (0.98 ± 0.05)	0.38 ± 0.02 (0.39 ± 0.02)
	Monoculture	0.42 ± 0.16^{aA}	0.09 ± 0.01^{aA}	1.04 ± 0.15	0.30 ± 0.03
Arenosol (Vechta; 2018—Rye; 2019—Corn)	Monoculture	0.21 ± 0.08	0.07 ± 0.02	0.63 ± 0.08	0.30 ± 0.02

Note. For each site, means with different lowercase letters indicate significant differences between the monoculture and sampling locations within the agroforestry (linear mixed-effect models with Fisher's least significant difference test at $P \leq 0.05$). The different uppercase letters indicate significant differences between the monoculture and agroforestry as a whole, weighted by the areal coverage of the tree row and crop row sampling locations (linear mixed-effect models with Fisher's least significant difference test at $P \leq 0.05$). For agroforestry, the first values are area-weighted by the tree row, and at 1 and 7 m distances from the tree row; the second values in parentheses include the 24 m distance in area-weighting (see Section 2.2). The site with the Arenosol soil was a cropland monoculture during the measurement period. Annual fluxes from March 2018 to February 2019 were not tested statistically for differences between agroforestry and monoculture since these values are trapezoidal extrapolations. Annual fluxes on mass-basis were converted into area-basis using the averaged soil bulk density in the top 5 cm measured at each site.

3.3. Denitrification Gene Abundance

Among the denitrification genes, *nirK* (encoding for NO_2^- reductase) was the most abundant. The abundance of *nirK* gene decreased with increasing distance from the tree row into the crop row of the agroforestry systems and was lowest in the monoculture systems ($P \leq 0.013$; Table 4). The abundance of *nirS* gene (encoding for NO_2^- reductase) followed a similar spatial pattern as *nirK* among sampling locations ($P \leq 0.004$; Table 4). The abundance of *nosZ* clade I gene (encoding for N_2O reductase) was comparable between the agroforestry and monoculture in the Phaeozem soil (Table 4). In the Cambisol soil, *nosZ* clade I gene abundance was higher in the tree row than in the crop row of the agroforestry ($P < 0.001$; Table 4) but comparable to the cropland monoculture ($P = 0.07$; Table 4). The abundance of *nosZ* clade II gene (encoding for N_2O reductase) did not differ among sampling locations in the Phaeozem and Cambisol soils ($P \geq 0.13$; Table 4).

3.4. Temporal Relationships Between Gross N_2O Fluxes and Soil Factors

Gross N_2O emissions rather than gross N_2O uptake strongly determined net N_2O flux either across the three study sites (Figure 3a) or separately for each management system (Table 5). Across sites, gross N_2O emissions were influenced by total mineral N (Figure 3b) and soil respiration (Table S4 in Supporting Information S1). Although soil temperature showed a correlation with gross N_2O emissions, this was not solely by temperature but also by its autocorrelation with total mineral N and soil respiration (Table S4 in Supporting Information S1). Considering the variables that were not autocorrelated with each other (Table S4 in Supporting Information S1), the best predictive relationships for gross N_2O emissions from the agroforestry were total mineral N and soil respiration. Separating between the tree and crop rows of the agroforestry, total mineral N was the best predictor (or the limit-

Table 3
Mean (±SE, n = 4 Plots for the Phaeozem and Cambisol Soils, n = 8 Plots for the Arenosol Soil) Water Content, Soil Respiration, Mineral N, Microbial Biomass N and C Across Monthly Measurements From March 2018 to September 2019 in the Top 5-cm Depth at Three Sites of Cropland Agroforestry and Cropland Monocultures in Germany

Soil type (site)	Management system	Water-filled pore space (%)	Soil respiration (mg CO_2-C kg^{-1} h^{-1})	Total mineral N (mg kg^{-1})	Microbial biomass N (mg kg^{-1})	Microbial biomass C (mg kg^{-1})
Phaeozem (Dornburg)	Agroforestry					
	Tree row	47 ± 4^{a}	1.3 ± 0.2^{a}	4 ± 1^{day}	91 ± 9^{a}	573 ± 39^{a}
	1 m crop row	42 ± 3^{a}	0.9 ± 0.1^{bc}	12 ± 3^{c}	66 ± 8^{bc}	492 ± 49^{ab}
	7 m crop row	42 ± 2^{a}	1.1 ± 0.2^{ab}	24 ± 8^{bc}	69 ± 7^{ab}	474 ± 36^{b}
	24 m crop row	42 ± 2^{a}	1.0 ± 0.2^{ab}	63 ± 22^{a}	54 ± 16^{c}	377 ± 37^{c}
	Monoculture	34 ± 2^{b}	0.6 ± 0.1^{c}	38 ± 14^{ab}	81 ± 6^{ab}	565 ± 29^{a}
Cambisol (Wendhausen)	Agroforestry					
	Tree row	47 ± 3^{a}	0.7 ± 0.1^{a}	4 ± 1^{b}	108 ± 8^{a}	570 ± 110^{a}
	1 m crop row	41 ± 2^{b}	0.5 ± 0.1^{b}	30 ± 7^{a}	106 ± 29^{ab}	448 ± 51^{ab}
	7 m crop row	40 ± 2^{b}	0.5 ± 0.1^{b}	42 ± 12^{a}	64 ± 16^{b}	372 ± 53^{b}
	24 m crop row	41 ± 2^{b}	0.5 ± 0.1^{b}	39 ± 11^{a}	74 ± 14^{ab}	352 ± 74^{b}
	Monoculture	35 ± 2^{c}	0.4 ± 0.1^{b}	42 ± 12^{a}	75 ± 23^{ab}	311 ± 53^{b}
Arenosol (Vechta)	Monoculture	30 ± 3	0.7 ± 0.2	29 ± 14	33 ± 7	217 ± 22

Note. For each site, means with different lowercase letters indicate significant differences between the monoculture and sampling locations within the agroforestry (linear mixed-effect models with Fisher's least significant difference test at $P \leq 0.05$).

ing factor) for gross N_2O emissions from tree rows whereas both total mineral N and WFPS regulated the gross N_2O emissions from the crop rows (Table 5). For the monocultures, total mineral N, soil respiration (which was lowest in monocultures; Table 3), and WFPS regulated the gross N_2O emissions (Table 5). We did not detect any significant correlations between gross N_2O emissions and the denitrification gene abundance.

Table 4
Mean (±SE, n = 4 Plots for the Phaeozem and Cambisol Soils, n = 8 Plots for the Arenosol Soil) Denitrification Gene Abundances (NirK, NirS, NosZ Clade I, NosZ Clade II) Across Monthly Measurements From March 2018 to September 2019 in the Top 5-cm Depth at Three Sites of Cropland Agroforestry and Cropland Monocultures in Germany

		nirK	*nirS*	*nosZ* clade I	*nosZ* clade II
Soil type (site)	Management system	(1×10^8 gene copy number g^{-1} dry soil)			
Phaeozem (Dornburg)	Agroforestry				
	Tree row	15.8 ± 2.4^{a}	0.9 ± 0.1^{a}	1.3 ± 0.2^{a}	2.4 ± 0.4^{a}
	1 m crop row	10.8 ± 1.2^{b}	1.6 ± 0.5^{a}	0.9 ± 0.1^{a}	2.7 ± 0.3^{a}
	7 m crop row	11.1 ± 1.4^{b}	0.7 ± 0.1^{ab}	1.0 ± 0.1^{a}	2.6 ± 0.3^{a}
	24 m crop row	10.5 ± 1.7^{b}	0.6 ± 0.1^{b}	1.0 ± 0.2^{a}	2.5 ± 0.3^{a}
	Monoculture	9.4 ± 1.2^{b}	0.6 ± 0.1^{ab}	1.2 ± 0.2^{a}	2.1 ± 0.2^{a}
Cambisol (Wendhausen)	Agroforestry				
	Tree row	10.9 ± 1.9^{a}	1.1 ± 0.2^{a}	2.3 ± 0.4^{a}	1.5 ± 0.3^{a}
	1 m crop row	4.7 ± 0.7^{b}	0.7 ± 0.1^{b}	1.3 ± 0.2^{bc}	1.1 ± 0.2^{a}
	7 m crop row	4.3 ± 1.0^{b}	0.6 ± 0.1^{b}	1.3 ± 0.2^{c}	1.1 ± 0.2^{a}
	24 m crop row	4.2 ± 0.7^{b}	0.6 ± 0.1^{b}	1.2 ± 0.2^{c}	0.9 ± 0.2^{a}
	Monoculture	3.9 ± 0.6^{b}	0.5 ± 0.1^{b}	1.7 ± 0.2^{ab}	0.9 ± 0.1^{a}

Note. For each site, means with different lowercase letters indicate significant differences between the monoculture and sampling locations within the agroforestry (linear mixed-effect models with Fisher's least significant difference test at $P \leq 0.05$).

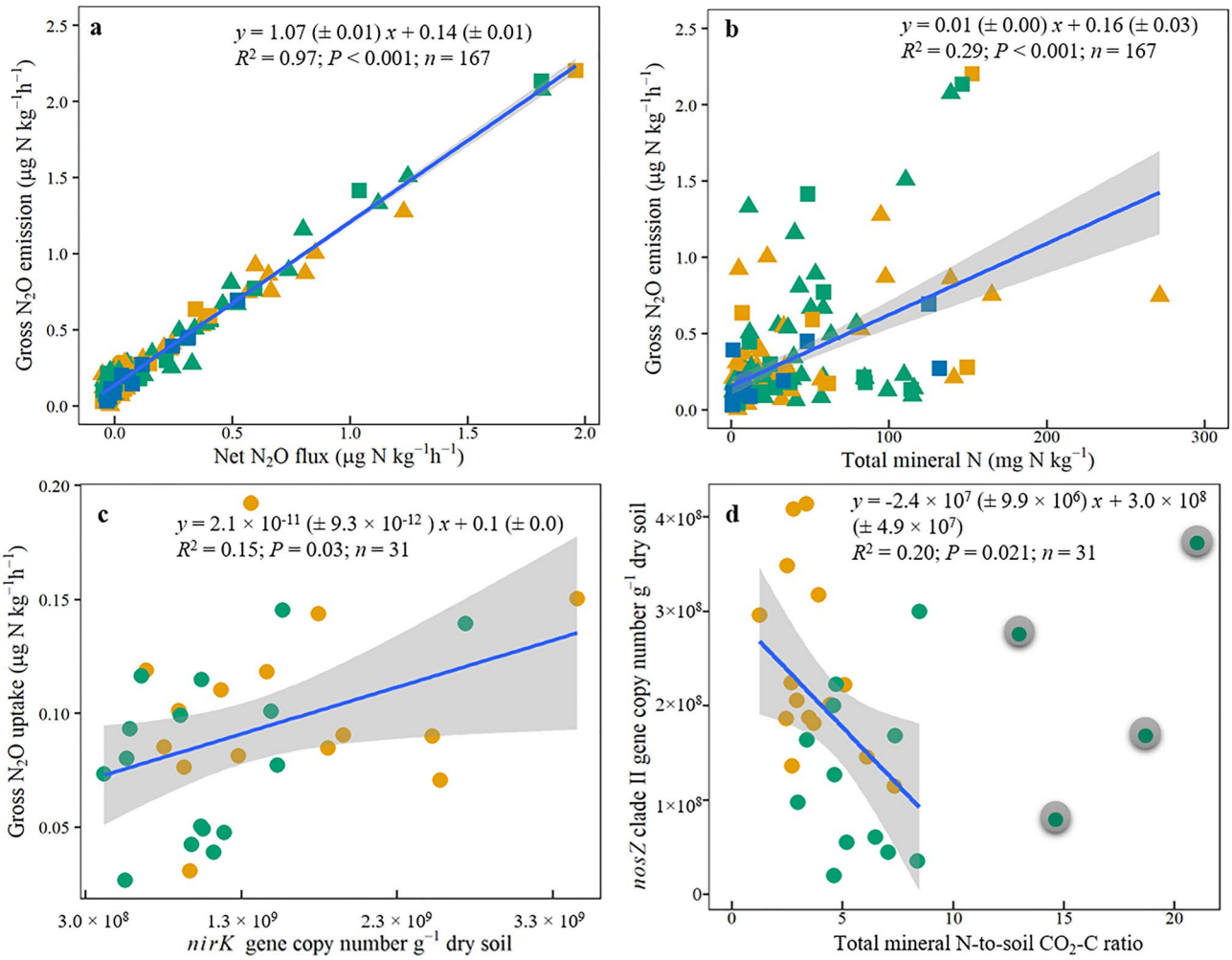

Figure 3. Cropland agroforestry and monocultures over 1.5 years of measurements: regression (parameter estimates ± 95% confidence interval) of gross N_2O emission with net N_2O flux (a) and total mineral N (b) across three sites. Agroforestry tree rows over 1.5 years of measurements: regressions between gross N_2O uptake and *nirK* gene abundance (c), and between *nosZ* clade II gene abundance and mineral N-to-soil CO_2-C ratio (d, including only ratios <10). Each data point is a monthly mean of four (in Phaeozem and Cambisol soils) or eight replicate plots (in Arenosol soil). Tree row (●), crop row (1-m, 7-m, 24-m sampling locations, (▲), monoculture (■), Phaeozem soil (●), Cambisol soil (●), Arenosol soil (●).

On the other hand, there were no significant correlations between gross N_2O uptake and any of the measured soil variables either across sites or separately for agroforestry and monoculture systems. However, considering only the tree rows of the agroforestry, gross N_2O uptake was correlated with *nirK* gene abundance (Figure 3c), which was also linked with the *nosZ* clade II gene abundance (Pearson's $r = 0.62$, $P < 0.001$, $n = 31$). The *nosZ* clade II gene abundance was negatively correlated to mineral N-to-soil CO_2-C ratio, particularly when ratios were less than 10 (Figure 3d).

4. Discussion

4.1. Gross N_2O Emissions

To date, gross N_2O fluxes had not yet been systematically compared between cropland agroforestry and monoculture, and our study uniquely linked gross N_2O fluxes with denitrification gene abundance in addition to the commonly measured soil controlling factors. In the agroforestry tree rows, the high WFPS (Table 3), high abundance of denitrification genes (Table 4) and low mineral N-to-soil CO_2-C ratio would have favored enhanced gross N_2O emission (Yang & Silver, 2016a). The latter, that is, low mineral N-to-soil CO_2-C ratio (of which heterotrophic respiration from available C can account for 70–85%; Chen et al., 2019; Van Straaten et al., 2011;

Table 5
Multiple Regressions Between Gross N_2O Emission and Soil Factors (Which are Not Autocorrelated With Each Other) Separately for Cropland Agroforestry and Monoculture, and the Relationships Between Gross and Net N_2O Fluxes

Management systems	*n*	Regression equations	*P* Value	R^2
Agroforestry	124	Gross N_2O emission = 0.004(±0.001) × total mineral N + 0.132(±0.044) × soil respiration + 0.072(±0.045)	<0.001	0.32
Tree row	31	Gross N_2O emission = 0.017(±0.005) × total mineral N + 0.056(±0.023)	0.002	0.28
Crop row	93	Gross N_2O emission = 0.004(±0.001) × total mineral N + 0.009(±0.004) × WFPS − 0.159(±0.168)	<0.001	0.26
Monoculture	43	Gross N_2O emission = 0.006(±0.001) × total mineral N + 0.019(±0.008) × WFPS + 0.271(±0.121) × soil respiration − 0.677(±0.286)	<0.001	0.49
Between gross and net N_2O fluxes				
Agroforestry	124	Gross N_2O emission = 1.048(±0.018) × net N_2O flux	<0.001	0.96
Tree row	31	Gross N_2O emission = 1.473(±0.381) × net N_2O flux	<0.001	0.34
Crop row	93	Gross N_2O emission = 1.045(±0.020) × net N_2O flux	<0.001	0.97
Monoculture	43	Gross N_2O emission = 1.103(±0.018) × net N_2O flux	<0.001	0.99

Zhang et al., 2013), favors for N_2O-to-N_2 reduction during high WFPS conditions (Weier et al., 1993); this last step of the denitrification process is included in the quantification of gross N_2O emission by $^{15}N_2O$ PD technique (Wen et al., 2016). Thus, the low gross N_2O emissions from the agroforestry tree rows (Table 2) indicated the overriding influence of its low mineral N levels (Table 3). Indeed, in the agroforestry tree rows, the only soil factor correlating with gross N_2O emissions was mineral N (Table 5), suggesting that this substrate as electron acceptor limited the production of N_2O rather than the electron donor (as reflected by the high soil CO_2 that partly includes heterotrophic respiration of available C as well as by the high microbial C in the tree row; Table 3). Similar findings were reported for beech and spruce stands in Germany, whereby NO_3^- levels predominantly regulate soil gross N_2O emissions (Wen et al., 2017). In contrast, the larger gross N_2O emissions from the crop rows were mirrored with their larger ratios of mineral N-to-soil CO_2-C while WFPS remained high (Table 3); this signified the secondary control of WFPS once N availability was increased by fertilization at the crop row (Table 5). At our study sites, the high WFPS in the agroforestry (Table 3) has been attributed to the reduction of wind speed by trees (Kanzler et al., 2019; Swieter et al., 2019) and thereby lowering evapotranspiration (Markwitz et al., 2020).

Across agroforestry tree and crop rows at two sites, the positive relationship of gross N_2O emissions with mineral N (Table 5 and Table S4 in Supporting Information S1) reflected their similar patterns from the tree to the crop rows (Tables 2 and 3). The positive relationship of gross N_2O emissions with soil CO_2 largely depicted the parallel patterns of these variables between these two sites (Phaeozem > Cambisol; Tables 2 and 3). The effect of soil temperature was only indirect in that it was autocorrelated with mineral N and soil respiration (Table S4 in Supporting Information S1). For example, soil temperature increased from spring, when fertilization occurred (Figures S3d and S3e in Supporting Information S1), to summer and decreased toward fall, which also reflected the seasonal pattern of soil respiration (Figures S3g and S3h in Supporting Information S1). Altogether, the benefit of agroforestry tree rows in controlling gross N_2O emissions was largely on reduced electron acceptor (mineral N) relative to electron donor (as reflected partly by the soil CO_2 and microbial C), since WFPS and denitrification gene abundance were favorably large in the tree rows (Tables 3 and 4; see Section 4.2).

In cropland monocultures, the temporal variations of gross N_2O emissions were mirrored with seasonal changes in substrate availability and soil aeration (Table 5). The pulse N_2O emissions following one-time N fertilization to corn during spring (Figures 2b and 2c) with high WFPS and temperature (Figures S3b and S3c, S3e and S3f in Supporting Information S1) may be attributed to low N uptake of corn seedlings at the start of the growing season; indeed, soil mineral N in spring was higher than in summer when N uptake was probably substantial as the corn grew. Yang and Silver (2016b) reported for corn cropland that plant uptake of N indirectly regulates gross N_2O emissions. When our studied croplands had winter wheat and spring N fertilization was staggered (split in 2–3 applications; Figures 2a and 2b), the pulses of gross N_2O emissions were not as high as those when the crop was corn, possibly because winter wheat had an early growth start that stimulated N uptake in spring. When the crop was barley, spring N fertilization rate was the lowest (Table 1), and gross N_2O emissions in spring were not as high as those in the above crops (Figure 2a). These fertilization practices, as practiced by farmers for

these crops, reflected the pattern of soil mineral N levels at these sites. Moreover, the influence of soil respiration on gross N_2O emissions from monocultures (Table 5) was exhibited through its similarity in seasonal patterns with soil temperature (Figures S3d–S3i in Supporting Information S1), indicating soil CO_2-C increased from spring to summer and decreased toward fall. The regulation of WFPS on gross N_2O emissions from monocultures (Table 5) was related to the differences in soil textures of our study sites (Table S1 in Supporting Information S1) with the fine-textured soils (Phaeozem and Cambisol) exhibiting larger WFPS than the sandy Arenosol soil (Table 3 and Figures S3a–S3c in Supporting Information S1). It should also be noted that 2018 had a lower precipitation than the 10-year average (Table 1), and the monoculture (without the wind reduction from trees as that in agroforestry; Markwitz et al., 2020) had the lowest WFPS (Table 3 and Figures S3a–S3c in Supporting Information S1); this may have a dampening effect on gross N_2O emissions as otherwise may occur in years with normal precipitation. Therefore, in addition to precipitation, management practices (fertilization, crops) and soil texture, which influenced mineral N and WFPS at a local scale, were large-scale controllers of gross N_2O emissions from monocultures.

The whole (area-weighted for tree and crop rows) agroforestry tended to have less annual gross N_2O emissions than the monocultures (average reductions of 6% in the Cambisol soil and 36% in the Phaeozem soil; Table 2) although the tree rows only occupied 20% of the agroforestry area. The predominant control of mineral N on gross N_2O emissions across agroforestry and monoculture systems (Table 5 and Figure 3b) reflected the clear benefit from unfertilized tree rows on reducing gross N_2O emissions, especially that gross N_2O emissions were the main determinant of net N_2O emissions from the soils (Table 5 and Figure 3a). This also suggests for optimal adjustments of the areal coverages between tree and crop rows to optimize benefits between provision (e.g., food, biomass, soil nutrients) and regulation functions (e.g., GHG, water quality).

4.2. Denitrification Gene Abundance

The increased microbial biomass in the agroforestry tree rows at our sites (Table 3) agreed with molecular studies that found promotion of microbial population size in the tree rows as compared to the crop rows or monoculture croplands in temperate regions (Banerjee et al., 2016; Beule et al., 2020). A much detailed molecular quantification of the microbial population at our study sites showed that the tree rows not only increase the bacterial and fungal population as well as denitrification gene abundance (Beule et al., 2020) but also alter the community composition of soil microorganisms (Beule et al., 2021; Beule & Karlovsky, 2021), implying changes in microbial community functions. However, denitrifier population size may only represent the genetic potential for denitrification rather than a reliable predictor of soil N_2O fluxes, which explained the contrasting spatial patterns of denitrification gene abundance and gross N_2O emissions between agroforestry tree and crop rows or monoculture (Tables 2 and 4). Similar opposing findings of denitrification gene abundance and net N_2O fluxes were reported from field studies in temperate croplands (Dandie et al., 2008) and sclerophyll forest (Liu et al., 2013). Denitrification is a facultative physiological trait since all known denitrifying bacteria are capable of aerobic respiration (Chen & Strous, 2013). Denitrifier abundance may become a limiting factor for gross N_2O emissions when substrate levels and anaerobic conditions already prevail. Thus, it was not surprising that in the tree rows, N availability (Table 5) rather than denitrifier population size controlled gross N_2O emissions. This conflicts with the assumption that the functional gene abundance of microorganisms can serve as a predictor of soil process rates. Although links between gene abundance and soil processes are frequently reported, a significant part of these studies is conducted under controlled laboratory conditions (e.g., Chen et al., 2020), ignoring the complexity of conditions occurring in the field. We, therefore, question to which extent results obtained from laboratory incubation studies can predict the actual processes occurring under field conditions. We argue that extensive field rather than laboratory studies are essential to understand the interactions between soil microbial communities and the processes they carry out.

4.3. Gross N_2O Uptake

The increased gross N_2O uptake in the agroforestry tree rows in the Phaeozem soil (Table 2) was paralleled with low mineral N-to-soil CO_2-C ratio and high WFPS, which concurred with earlier findings (Wen et al., 2017; Yang & Silver, 2016a). At this site, the high WFPS and soil CO_2 (which partly indicated high heterotrophic respiration of available C; Chen et al., 2019; Van Straaten et al., 2011; Zhang et al., 2013) in the tree row would favor for reduction of N_2O to N_2, resulting in higher gross N_2O uptake in the agroforestry relative to the monoculture

(Table 2). The positive correlation of gross N_2O uptake with *nirK* gene abundance in agroforestry tree rows across two sites (Figure 3c) suggests that in a condition of low mineral N with high available C (e.g., high soil CO_2 and microbial C) and WFPS (Table 3) denitrifiers could not gain enough energy from only NO_2^--to-N_2O reduction, and thus completed the final step of denitrification, N_2O-to-N_2 reduction. The latter was further supported by the increasing *nosZ* clade II gene abundance with decreasing mineral N-to-soil CO_2-C ratio (Figure 3d), indicating that the ratio of mineral N-to-soil CO_2-C (Phaeozem < Cambisol soil) could be the underlying factor driving the difference in gross N_2O uptake in the tree rows between the two sites (Phaeozem > Cambisol soil) through its effect on the population size of *nosZ* clade II (Phaeozem > Cambisol soil). Annual gross N_2O uptake in the agroforestry system tended to increase by 27% (Cambisol soil) to 42% (Phaeozem soil) compared to the monocultures (Table 2). Collectively, the practical merit of trees in the agroforestry system, with regard to enhanced gross N_2O uptake, was mainly through an increase in C availability (as reflected partly by soil respiration and microbial C; Table 3) with an absence of fertilization.

5. Implications

Our sites of cropland agroforestry and monocultures have been shown to display nutrient saturation (Schmidt et al., 2021). As mineral N predominantly controlled gross N_2O emissions (which in turn influenced net soil N_2O emissions) from both agroforestry and monocultures, our findings suggest that if fertilizer inputs are optimized without sacrificing crop yield or profit, combined with the impact of tree rows on increased N_2O uptake, agroforestry will be an efficient mitigation strategy to curb N_2O emissions from croplands. From the aspect of economic performance, less investment in fertilizer inputs associated with environmental benefits (e.g., reduced N_2O emissions) and diversified sources of income (crop yield, biofuel feedstock from tree biomass) would improve the profitability of agroforestry and facilitate its adoption by farmers. Overall, the GHG regulation function of the agroforestry system should be considered in the economic and ecological valuation to support its policy implementation (Kay et al., 2019).

Data Availability Statement

The data of this study are available from the BonaRes Data Centre repository (https://doi.org/10.20387/bonares-x13m-z796).

Acknowledgments
This work was funded by the Bundesministerium für Bildung und Forschung (Bonares-SIGNAL project, 031A562A/031B0510A/031B1063A). Jie Luo was supported by China Scholarship Council. We thank Julia Morley, Helena Römer, Selena Algermissen, Antje Sophie Makowski, Andrea Bauer, Kerstin Langs, Dirk Böttger, and Martina Knaust for all the field and laboratory assistance. Open access funding enabled and organized by Projekt DEAL.

References

Almaraz, M., Wong, M. Y., & Yang, W. H. (2020). Looking back to look ahead: A vision for soil denitrification research. *Ecology*, *101*(1), e02917. https://doi.org/10.1002/ecy.2917

Amadi, C. C., Farrell, R. E., & van Rees, K. C. (2017). Greenhouse gas emissions along a shelterbelt-cropped field transect. *Agriculture, Ecosystems & Environment*, *241*, 110–120. https://doi.org/10.1016/j.agee.2016.09.037

Amadi, C. C., van Rees, K. C., & Farrell, R. E. (2016). Soil-atmosphere exchange of carbon dioxide, methane and nitrous oxide in shelterbelts compared with adjacent cropped fields. *Agriculture, Ecosystems & Environment*, *223*, 123–134. https://doi.org/10.1016/j.agee.2016.02.026

Banerjee, S., Baah-Acheamfour, M., Carlyle, C. N., Bissett, A., Richardson, A. E., Siddique, T., et al. (2016). Determinants of bacterial communities in Canadian agroforestry systems. *Environmental Microbiology*, *18*(6), 1805–1816. https://doi.org/10.1111/1462-2920.12986

Beaudette, C., Bradley, R. L., Whalen, J. K., McVetty, P., Vessey, K., & Smith, D. L. (2010). Tree-based intercropping does not compromise canola (*Brassica napus* L.) seed oil yield and reduces soil nitrous oxide emissions. *Agriculture, Ecosystems & Environment*, *139*(1–2), 33–39. https://doi.org/10.1016/j.agee.2010.06.014

Beule, L., Arndt, M., & Karlovsky, P. (2021). Relative abundances of species or sequence variants can be misleading: Soil fungal communities as an example. *Microorganisms*, *9*(3), 589. https://doi.org/10.3390/microorganisms9030589

Beule, L., Corre, M. D., Schmidt, M., Göbel, L., Veldkamp, E., & Karlovsky, P. (2019). Conversion of monoculture cropland and open grassland to agroforestry alters the abundance of soil bacteria, fungi and soil-N-cycling genes. *PLoS One*, *14*(6), 1–19. https://doi.org/10.1371/journal.pone.0218779

Beule, L., & Karlovsky, P. (2021). Tree rows in temperate agroforestry croplands alter the composition of soil bacterial communities. *PLoS One*, *16*(2), e0246919. https://doi.org/10.1371/journal.pone.0246919

Beule, L., Lehtsaar, E., Corre, M. D., Schmidt, M., Veldkamp, E., & Karlovsky, P. (2020). Poplar rows in temperate agroforestry croplands promote bacteria, fungi, and denitrification genes in soils. *Frontiers in Microbiology*, *10*, 1–5. https://doi.org/10.3389/fmicb.2019.03108

Beule, L., Lehtsaar, E., Rathgeb, A., & Karlovsky, P. (2019). Crop diseases and mycotoxin accumulation in temperate agroforestry systems. *Sustainability*, *11*(10), 2925. https://doi.org/10.3390/su11102925

Brandfass, C., & Karlovsky, P. (2008). Upscaled CTAB-based DNA extraction and real-time PCR assays for *Fusarium culmorum* and *F. graminearum* DNA in plant material with reduced sampling error. *International Journal of Molecular Sciences*, *9*(11), 2306–2321. https://doi.org/10.3390/ijms9112306

Brookes, P. C., Landman, A., Pruden, G., & Jenkinson, D. S. (1985). Chloroform fumigation and the release of soil nitrogen: A rapid direct extraction method to microbial biomass nitrogen in soil. *Soil Biology and Biochemistry*, *17*(6), 837–842. https://doi.org/10.1016/0038-0717(85)90144-0

Butterbach-Bahl, K., Baggs, E. M., Dannenmann, M., Kiese, R., & Zechmeister-Boltenstern, S. (2013). Nitrous oxide emissions from soils: How well do we understand the processes and their controls? *Philosophical Transactions of the Royal Society of London. Series B, Biological Sciences*, *368*(1621), 20130122. https://doi.org/10.1098/rstb.2013.0122

Butterbach-Bahl, K., Willibald, G., & Papen, H. (2002). Soil core method for direct simultaneous determination of N_2 and N_2O emissions from forest soils. *Plant and Soil*, *240*(1), 105–116. https://doi.org/10.1023/A:1015870518723

Chapman, M., Walker, W. S., Cook-Patton, S. C., Ellis, P. W., Farina, M., Griscom, B. W., & Baccini, A. (2020). Large climate mitigation potential from adding trees to agricultural lands. *Global Change Biology*, *26*(8), 4357–4365. https://doi.org/10.1111/gcb.15121

Chapuis-Lardy, L., Wrage, N., Metay, A., Chotte, J.-L., & Bernoux, M. (2007). Soils, a sink for N_2O? A review. *Global Change Biology*, *13*(1), 1–17. https://doi.org/10.1111/j.1365-2486.2006.01280.x

Chen, F., Yan, G., Xing, Y., Zhang, J., Wang, Q., Wang, H., et al. (2019). Effects of N addition and precipitation reduction on soil respiration and its components in a temperate forest. *Agricultural and Forest Meteorology*, *271*, 336–345. https://doi.org/10.1016/j.agrformet.2019.03.021

Chen, J., & Strous, M. (2013). Denitrification and aerobic respiration, hybrid electron transport chains and co-evolution. *Biochimica et Biophysica Acta*, *1827*(2), 136–144. https://doi.org/10.1016/j.bbabio.2012.10.002

Chen, Y., Liu, F., Kang, L., Zhang, D., Kou, D., Mao, C., et al. (2020). Large-scale evidence for microbial response and associated carbon release after permafrost thaw. *Global Change Biology*, *27*(14), 3218–3229. https://doi.org/10.1111/gcb.15487

Crawley, M. J. (2007). *The R Book*. Chinchester, UK: John Wiley & Sons Ltd.

Dandie, C. E., Burton, D. L., Zebarth, B. J., Henderson, S. L., Trevors, J. T., & Goyer, C. (2008). Changes in bacterial denitrifier community abundance over time in an agricultural field and their relationship with denitrification activity. *Applied and Environmental Microbiology*, *74*(19), 5997–6005. https://doi.org/10.1128/AEM.00441-08

Davidson, E. A., Keller, M., Erickson, H. E., Verchot, L. V., & Veldkamp, E. (2000). Testing a conceptual model of soil emissions of nitrous and nitric oxides. *BioScience*, *50*(8), 667. https://doi.org/10.1641/0006-3568(2000)050[0667:TACMOS]2.0.CO;2

Foley, J. A., Ramankutty, N., Brauman, K. A., Cassidy, E. S., Gerber, J. S., Johnston, M., et al. (2011). Solutions for a cultivated planet. *Nature*, *478*(7369), 337–342. https://doi.org/10.1038/nature10452

Galloway, J. N., Townsend, A. R., Erisman, J. W., Bekunda, M., Cai, Z., Freney, J. R., et al. (2008). Transformation of the nitrogen cycle: Recent trends, questions, and potential solutions. *Science*, *320*(5878), 889–892. https://doi.org/10.1126/science.1136674

Guerra, V., Beule, L., Lehtsaar, E., Liao, H.-L., & Karlovsky, P. (2020). Improved protocol for DNA extraction from subsoils using phosphate lysis buffer. *Microorganisms*, *8*(4), 532. https://doi.org/10.3390/microorganisms8040532

IPCC. (2014). Climate change 2014: Synthesis report. In R. K. Pachauri & L. A. Meyer (Eds.), *Contribution of working Groups I, II and III to the fifth assessment report of the intergovernmental panel on climate change [core Writing Team]* (p. 87). Geneva, Switzerland: IPCC. Retrieved from https://www.ipcc.ch/report/ar5/syr/

IPCC. (2019). *Climate change and land: An IPCC special report on climate change, desertification, land degradation, sustainable land management, food security, and greenhouse gas fluxes in terrestrial ecosystems* (pp. 551–672). Geneva, Switzerland: IPCC. Retrieved from https://www.ipcc.ch/srccl/chapter/chapter-6/

Juhanson, J., Hallin, S., Söderström, M., Stenberg, M., & Jones, C. M. (2017). Spatial and phyloecological analyses of *nosZ* genes underscore niche differentiation amongst terrestrial N_2O reducing communities. *BioScience*, *115*, 82–91. https://doi.org/10.1016/j.soilbio.2017.08.013

Kanzler, M., Böhm, C., Mirck, J., Schmitt, D., & Veste, M. (2019). Microclimate effects on evaporation and winter wheat (*Triticum aestivum* L.) yield within a temperate agroforestry system. *Agroforestry Systems*, *93*(5), 1821–1841. https://doi.org/10.1007/s10457-018-0289-4

Kay, S., Graves, A., Palma, J. H., Moreno, G., Roces-Díaz, J. V., Aviron, S., et al. (2019). Agroforestry is paying off—Economic evaluation of ecosystem services in European landscapes with and without agroforestry systems. *Ecosystem Services*, *36*, 100896. https://doi.org/10.1016/j.ecoser.2019.100896

Koehler, B., Corre, M. D., Veldkamp, E., Wullaert, H., & Wright, S. J. (2009). Immediate and long-term nitrogen oxide emissions from tropical forest soils exposed to elevated nitrogen input. *Global Change Biology*, *15*(8), 2049–2066. https://doi.org/10.1111/j.1365-2486.2008.01826.x

Lang, M., Li, P., Ti, C., Zhu, S., Yan, X., & Chang, S. X. (2019). Soil gross nitrogen transformations are related to land-uses in two agroforestry systems. *Ecological Engineering*, *127*, 431–439. https://doi.org/10.1016/j.ecoleng.2018.12.022

Langenberg, J., Feldmann, M., & Theuvsen, L. (2018). Agroforestry systems: Using Monte-Carlo simulation for a risk analysis in comparison with arable farming systems. *German Journal of Agricultural Economics*, *67*, 95–112. https://doi.org/10.22004/AG.ECON.309977

Liu, X., Chen, C. R., Wang, W. J., Hughes, J. M., Lewis, T., Hou, E. Q., & Shen, J. (2013). Soil environmental factors rather than denitrification gene abundance control N_2O fluxes in a wet sclerophyll forest with different burning frequency. *BioScience*, *57*, 292–300. https://doi.org/10.1016/j.soilbio.2012.10.009

Ma, Z., Chen, H. Y. H., Bork, E. W., Carlyle, C. N., & Chang, S. X. (2020). Carbon accumulation in agroforestry systems is affected by tree species diversity, age and regional climate: A global meta-analysis. *Global Ecology and Biogeography*, *29*(10), 1817–1828. https://doi.org/10.1111/geb.13145

Markwitz, C., Knohl, A., & Siebicke, L. (2020). Evapotranspiration over agroforestry sites in Germany. *Biogeosciences*, *17*(20), 5183–5208. https://doi.org/10.5194/bg-17-5183-2020

Matson, A. L., Corre, M. D., Langs, K., & Veldkamp, E. (2017). Soil trace gas fluxes along orthogonal precipitation and soil fertility gradients in tropical lowland forests of Panama. *Biogeosciences*, *14*(14), 3509–3524. https://doi.org/10.5194/bg-14-3509-2017

Mitchell, E., Scheer, C., Rowlings, D., Cotrufo, M. F., Conant, R. T., Friedl, J., & Grace, P. (2020). Trade-off between 'new' SOC stabilisation from above-ground inputs and priming of native C as determined by soil type and residue placement. *Biogeochemistry*, *149*(2), 221–236. https://doi.org/10.1007/s10533-020-00675-6

Müller, C., & Sherlock, R. R. (2004). Nitrous oxide emissions from temperate grassland ecosystems in the Northern and Southern Hemispheres. *Global Biogeochemical Cycles*, *18*, GB1045. https://doi.org/10.1029/2003GB002175

Pardon, P., Reubens, B., Mertens, J., Verheyen, K., de Frenne, P., de Smet, G., et al. (2018). Effects of temperate agroforestry on yield and quality of different arable intercrops. *Agricultural Systems*, *166*, 135–151. https://doi.org/10.1016/j.agsy.2018.08.008

Pardon, P., Reubens, B., Reheul, D., Mertens, J., de Frenne, P., Coussement, T., et al. (2017). Trees increase soil organic carbon and nutrient availability in temperate agroforestry systems. *Agriculture, Ecosystems & Environment*, *247*, 98–111. https://doi.org/10.1016/j.agee.2017.06.018

R Core Team. (2019). *R: A language and environment for statistical computing*. Vienna, Austria: R Foundation for Statistical Computing. Retrieved from https://www.r-project.org/

Schmidt, M., Corre, M. D., Kim, B., Morley, J., Göbel, L., Sharma, A. S. I., et al. (2021). Nutrient saturation of crop monocultures and agroforestry indicated by nutrient response efficiency. *Nutrient Cycling in Agroecosystems*, *119*(1), 69–82. https://doi.org/10.1007/s10705-020-10113-6

Shen, S. M., Pruden, G., & Jenkinson, D. S. (1984). PII: Mineralization and immobilization of nitrogen in fumigated soil and the measurement of microbial biomass nitrogen. *Soil Biology and Biochemistry*, *16*, 437–444. https://doi.org/10.1016/0038-0717(84)90049-X

Sihi, D., Davidson, E. A., Savage, K. E., & Liang, D. (2020). Simultaneous numerical representation of soil microsite production and consumption of carbon dioxide, methane, and nitrous oxide using probability distribution functions. *Global Change Biology*, *26*(1), 200–218. https://doi.org/10.1111/gcb.14855

Smith, J., Pearce, B. D., & Wolfe, M. S. (2013). Reconciling productivity with protection of the environment: Is temperate agroforestry the answer? *Renewable Agriculture and Food Systems*, *28*(1), 80–92. https://doi.org/10.1017/S1742170511000585

Strickland, M. S., Leggett, Z. H., Sucre, E. B., & Bradford, M. A. (2015). Biofuel intercropping effects on soil carbon and microbial activity. *Ecological Applications*, *25*(1), 140–150. https://doi.org/10.1890/14-0285.1

Swieter, A., Langhof, M., Lamerre, J., & Greef, J. M. (2019). Long-term yields of oilseed rape and winter wheat in a short rotation alley cropping agroforestry system. *Agroforestry Systems*, *93*(5), 1853–1864. https://doi.org/10.1007/s10457-018-0288-5

Tian, H., Yang, J., Xu, R., Lu, C., Canadell, J. G., Davidson, E. A., et al. (2018). Global soil nitrous oxide emissions since the preindustrial era estimated by an ensemble of terrestrial biosphere models: Magnitude, attribution, and uncertainty. *Global Change Biology*, *25*(2), 640–659. https://doi.org/10.1111/gcb.14514

Tsonkova, P., Böhm, C., Quinkenstein, A., & Freese, D. (2012). Ecological benefits provided by alley cropping systems for production of woody biomass in the temperate region: A review. *Agroforestry Systems*, *85*(1), 133–152. https://doi.org/10.1007/s10457-012-9494-8

Van Straaten, O., Veldkamp, E., & Corre, M. D. (2011). Simulated drought reduces soil CO_2 efflux and production in a tropical forest in Sulawesi, Indonesia. *Ecosphere*, *2*(10), art119. https://doi.org/10.1890/ES11-00079.1

Veldkamp, E., Koehler, B., & Corre, M. D. (2013). Indications of nitrogen-limited methane uptake in tropical forest soils. *Biogeosciences*, *10*(8), 5367–5379. https://doi.org/10.5194/bg-10-5367-2013

Weier, K. L., Doran, J. W., Power, J. F., & Walters, D. T. (1993). Denitrification and the Dinitrogen/nitrous oxide ratio as affected by soil water, available carbon, and nitrate. *Proceedings of the National Academy of Sciences*, *57*(1), 66–72. https://doi.org/10.2136/sssaj1993.03615995005700010013x

Wen, Y., Chen, Z., Dannenmann, M., Carminati, A., Willibald, G., Kiese, R., et al. (2016). Disentangling gross N_2O production and consumption in soil. *Scientific Reports*, *6*, 36517. https://doi.org/10.1038/srep36517

Wen, Y., Corre, M. D., Schrell, W., & Veldkamp, E. (2017). Gross N_2O emission and gross N_2O uptake in soils under temperate spruce and beech forests. *Soil Biology and Biochemistry*, *112*, 228–236. https://doi.org/10.1016/j.soilbio.2017.05.011

Wolz, K. J., Lovell, S. T., Branham, B. E., Eddy, W. C., Keeley, K., Revord, R. S., et al. (2018). Frontiers in alley cropping: Transformative solutions for temperate agriculture. *Global Change Biology*, *24*(3), 883–894. https://doi.org/10.1111/gcb.13986

Yang, W. H., & Silver, W. L. (2016a). Gross nitrous oxide production drives net nitrous oxide fluxes across a salt marsh landscape. *Global Change Biology*, *22*(6), 2228–2237. https://doi.org/10.1111/gcb.13203

Yang, W. H., & Silver, W. L. (2016b). Net soil-atmosphere fluxes mask patterns in gross production and consumption of nitrous oxide and methane in a managed ecosystem. *Biogeosciences*, *13*(5), 1705–1715. https://doi.org/10.5194/bg-13-1705-2016

Yang, W. H., Teh, Y. A., & Silver, W. L. (2011). A test of a field-based ^{15}N-nitrous oxide pool dilution technique to measure gross N_2O production in soil. *Global Change Biology*, *17*(12), 3577–3588. https://doi.org/10.1111/j.1365-2486.2011.02481.x

Zhang, Q., Lei, H. M., & Yang, D. W. (2013). Seasonal variations in soil respiration, heterotrophic respiration and autotrophic respiration of a wheat and maize rotation cropland in the North China Plain. *Agricultural and Forest Meteorology*, *180*, 34–43. https://doi.org/10.1016/j.agrformet.2013.04.028

Zuur, A. F., Ieno, E. N., Walker, N., Saveliev, A. A., & Smith, G. M. (2009). *Mixed effects models and extensions in ecology with R. Statistics for Biology and Health*. New York: Springer.

References From the Supporting Information

Henry, S., Baudoin, E., López-Gutiérrez, J. C., Martin-Laurent, F., Brauman, A., & Philippot, L. (2004). Quantification of denitrifying bacteria in soils by *nirK* gene targeted real-time PCR. *Journal of Microbiological Methods*, *59*(3), 327–335. https://doi.org/10.1016/j.mimet.2004.07.002

Henry, S., Bru, D., Stres, B., Hallet, S., & Philippot, L. (2006). Quantitative detection of the *nosZ* gene, encoding nitrous oxide reductase, and comparison of the abundances of 16S rRNA, *narG, nirK*, and *nosZ* genes in soils. *Applied and Environmental Microbiology*, *72*(8), 5181–5189. https://doi.org/10.1128/AEM.00231-06

Jones, C. M., Graf, D. R. H., Bru, D., Philippot, L., & Hallin, S. (2013). The unaccounted yet abundant nitrous oxide-reducing microbial community: A potential nitrous oxide sink. *The ISME Journal*, *7*(2), 417–426. https://doi.org/10.1038/ismej.2012.125

Michotey, V., Méjean, V., & Bonin, P. (2000). Comparison of methods for quantification of cytochrome cd(1)-denitrifying bacteria in environmental marine samples. *Applied and Environmental Microbiology*, *66*(4), 1564–1571. https://doi.org/10.1128/AEM.66.4.1564-1571.2000

Throbäck, I. N., Enwall, K., Jarvis, A., & Hallin, S. (2004). Reassessing PCR primers targeting *nirS, nirK* and *nosZ* genes for community surveys of denitrifying bacteria with DGGE. *FEMS Microbiology Ecology*, *49*(3), 401–417. https://doi.org/10.1016/j.femsec.2004.04.011